The Influence of Blade Camber on the Performance of a Vertical Axis Wind Turbine in Fluctuating Wind

Michael D. Bausas, and Louis Angelo M. Danao, *Member, IAENG*

Abstract— **Vertical axis wind turbines (VAWTs) have been argued to possess many advantages over the horizontal axis wind turbines (HAWTs) that make them more suitable to complex terrain applications where wind conditions are inherently turbulent. However, due to the complexity of VAWT blade aerodynamics, the available literature on the subject are very limited, leaving a number of VAWT parameters such as λ, solidity, blade number, blade shape and camber to be optimized. Additionally, research on VAWT performance are mostly focused on uniform wind analysis rather than fluctuating. This paper aims to numerically simulate and compare the performance of a 5kW VAWT with cambered-airfoils under uniform and fluctuating wind conditions. The Reynolds averaged Navier-Stokes equations and k-ω SST model were applied through computational fluid dynamics modeling. Results revealed that the fluctuating wind induced detrimental effect to VAWT performance as the cycle-averaged unsteady power coefficient are lower than the optimum steady power coefficient at relatively the same order of tip speed ratio. Generally, the unsteady power coefficient greatly vary with the fluctuating wind and do not follow the steady performance curve of the VAWTs. Camber-bladed VAWT was found to perform better in unsteady wind case with cycle averaged power coefficient of 0.34 versus the straight-bladed VAWT with cycle averaged power coefficient of 0.31.**

Index Terms—**Camber, Unsteady Wind, VAWT, CFD**

I. Introduction

MAJORITY of research and development work is focused mainly on horizontal axis wind turbines (HAWTs), making it a more preferred technology than vertical axis wind turbines (VAWTs) in most large scale wind farms. HAWTs are more efficient aerodynamically than VAWTs but essentially require laminar wind flow or good quality wind energy [1,2]. Results from some recent studies have shown that VAWTs are theoretically more suitable for small scale power generation in urban terrain, where wind conditions are turbulent rather than uniform [2,3]. There are several claimed advantages of VAWTs over HAWTs that make them preferable for such conditions: ability to respond instantaneously to changing incoming wind direction; minimal performance degradation from turbulent wind flow; compact and simple design as some mechanical components can be situated at the base of the turbine, and maximum power coefficient (C_P) is achieved at low tip speed ratios (λ), thus reducing noise and safety issues.

Despite having the same order of C_P and numerous advantages over HAWT, VAWT still requires proper technology R&D to improve self-starting and optimize wind power extraction. A number of parameters still need to be optimized, such as λ, solidity, blade number, blade shape and, camber as well as constant or variable blade pitch offset [4]. However, due to the difficulty and complexity of modeling VAWT aerodynamics, related technical studies are scarce in literature which mostly deal with experimental and numerical analysis of VAWT performance under uniform wind conditions.

McIntosh et al. [5] investigated VAWT response when subjected to fluctuating free stream of sinusoidal nature while running at a constant rotational speed. Results showed that an increase in energy extraction can be attained using a rotational speed greater than the calculated steady state maximum. The over–speed control technique resulted in a 245% increase in energy extracted. Further improvements in the performance can be attained by using a tip speed ratio feedback controller incorporating time dependent effects of gust frequency and turbine inertia giving a further 42% increase in energy extraction. In his study, at low frequencies of fluctuation (0.05Hz) away from stall, the unsteady C_P closely tracks the steady C_P curve. While at higher frequencies (0.5Hz), the unsteady C_P is seen to form hysteresis loops with averages greater than steady predictions.

Scheurich and Brown [6] used vorticity transport model to investigate the aerodynamic performance and wake dynamics, both in uniform and fluctuating wind conditions, of three different vertical-axis wind turbines: straight-bladed configuration, curved-bladed configuration and helically twisted blades configuration. The turbines with non-twisted blades are shown to be somewhat less efficient than the turbine with helically twisted blades when the rotors are operated at constant rotational speed in unsteady wind conditions. In steady wind conditions, the power coefficients

that are produced by both the straight-bladed and curve-bladed turbines vary considerably within one rotor revolution because of the continuously varying angle of attack on the blades and, thus, the inherent unsteadiness in the blade aerodynamic loading. These variations are much larger, and thus far more significant, than those that are induced by the unsteadiness in the wind conditions.

Danao [7] conducted both experimental and numerical investigations of the effect of unsteady wind on the performance and aerodynamics of straight-bladed vertical axis wind turbine. Results of his study showed that periodically changing wind conditions can slightly improve the overall performance of VAWT when certain conditions are satisfied, such as: the mean tip speed ratio is just above the λ of the steady C_P maximum, the amplitude of fluctuation is small, and the frequency of fluctuation is high. Operation outside these defined conditions may cause the VAWT to run in λ bands with deep stall and vortex shedding or λ conditions that are drag dominated, to the detriment of the VAWT cycle–averaged C_P. Within realistic fluctuation frequencies, faster fluctuations marginally improve the performance of the VAWT.

Shahzad et al. [8] numerically analyzed the performance output of a VAWT that features 12 equally spaced rotor and stator blades respectively. The performance of the VAWT was monitored under an accelerated and decelerated gust of the value 1.09m/s² characterized by change in velocity from 4m/s to 10m/s. Results showed that the instantaneous torque output varies significantly when a gust of air is applied to the turbine. The torque outputs vary during accelerating and decelerating flows, highlighting the effect of transient phenomena. The abrupt change in the instantaneous torque output of the turbine may give rise to highly transient loads on the turbine's structure which may induce heavy stresses on the turbine leading to structural failure.

Kozak [4] developed an iterative procedure to optimize the VAWT's geometry using blade pitch in fluctuating wind conditions. Results of his study showed that power output could be raised at lower tip-speed ratios by mitigating the adverse effects of dynamic stall using blade pitch.

The aim of this study is to investigate the effect of blade camber on the overall performance of VAWT that is subjected to fluctuating wind speeds. To achieve this, two dimensional flow field around the VAWT was numerically simulated and analyzed through computational fluid dynamics (CFD) modeling. Results from the fluctuating wind simulations (torque and power variations), were compared between the camber-bladed VAWT and a symmetric-bladed counterpart.

II. METHODS

A. Numerical Model of VAWT

The 2-D computational domain was divided into two distinct sub-grids (as shown in Fig. 1)—a stationary sub-grid that is the rectangular outer zone, determining the overall calculation domain, with a circular opening centered on the turbine's rotational axis and a rotor sub-grid that is a circular inner zone, which shall rotate with rotor angular velocity.

The 2-D VAWT model was designed without the blade-support arm and blade ends, hence neglecting their effect on rotor power extraction. Two VAWT configurations were considered in this study: one with NACA 0025 airfoils (symmetric) and the other with NACA 1425 (with blade camber) airfoils. Rotor diameter was set to 3m. The VAWT has three blades, each with a chord length of 0.15m.

All geometry and mesh of the model were generated using Ansys ICEM CFD. Each blade of the rotor was meshed with a total of 210 nodes, with clustering both in the leading and trailing edges where high gradients in pressure and flow were expected. The mesh was generated from an O-type block formed around the airfoil. The first cell height was set ensuring a y+ not exceeding 1. The cells expand from the wall to the O-type block boundaries with a growth rate of 1.1, giving a minimum of 90 layers within the said block. Cells beyond this block were set to have a maximum cell height not to exceed 0.10c for the rotor sub-grid, where c is the chord length of the airfoil. A smoothing algorithm was then applied to reduce the angle skewness of the cells (Fig. 2a).

One critical factor that dictates the overall quality of the computational domain is the spatial resolution of the mesh near the blade [7]. To optimize the model, parametric study of node density was carried out prior to actual unsteady wind simulations. The appropriate surface node density was determined by doing initial steady wind simulations wherein three surface node densities (70, 210 and 300 airfoil nodes) were tested at $\lambda = 4$. The blade torque coefficients in one full rotation for each case were compared. Results showed that while the torque curve of the mesh with 70 airfoil nodes greatly deviates from the curves of the other two cases, there is a very close agreement observed between the curves of the 210 and 300 airfoil nodes, such that they overlapped in most areas. The ΔC_P computed between these two cases was only 0.0025 or 0.825% difference in magnitude. Given this very minimal variance, the grid with 210 airfoil nodes was chosen since it can give accurate results as that with 300 nodes but at a lesser computational time.

The outer stationary sub-grid on the other hand, was meshed relatively coarser than the rotor sub-grid to reduce computational time. Minimum cell height was set to one chord length. Cell growth height from the circular interface to the wall boundaries was to 1.1 giving a maximum cell height of 0.25m. To avoid solid blockage and to allow full development of the wake, boundaries were positioned far enough from the rotor test section. The side boundaries and inlet distances were set to 5 diameters away from the rotor while outlet distance was set to 10 diameters away (Fig. 2b) as suggested for testing VAWT in open field scale [9].

The current symmetric and camber-bladed CFD models were validated with results of the QR5 wind tunnel test as cited by Scheurich et. al. [10] and the DMS model by Wahl [11]. As seen in Fig. 3, the current model compares well with the two other models in terms of the general trend of C_P

curve with optimum C_P occurring at λ = 3.5-4. Close results are observed between the current and Wahl's models, with minimal variation which can be attributed to the difference in numerical model used – DMS vs. CFD. On the other hand, though very similar trend was also observed from the results of the wind tunnel experiment of QR5, its relatively high C_P magnitudes may be due to its optimized blade configuration, which is helically twisted. Initial results also showed better performance of camber-bladed VAWT compared to its symmetric counterpart.
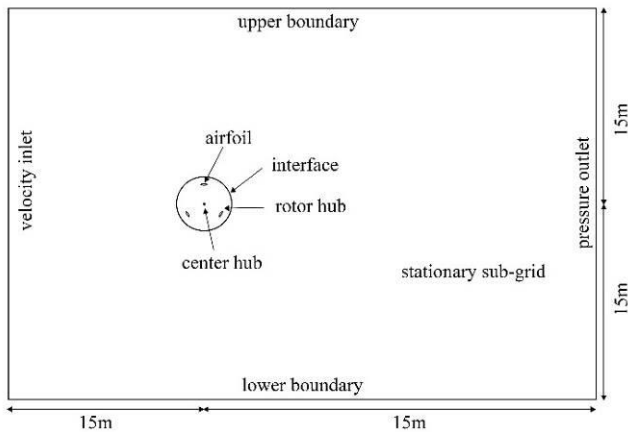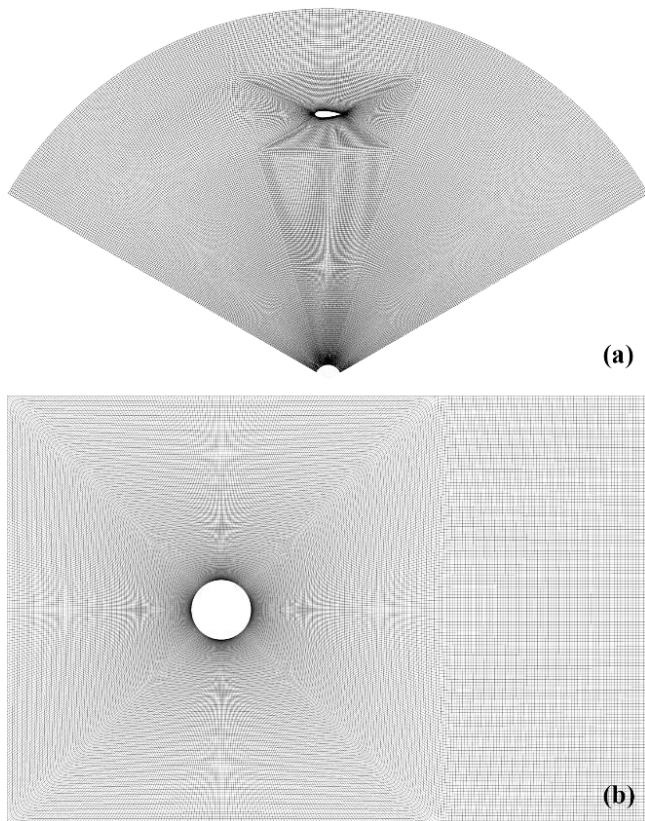

Fig. 1. 2-D computational model.

Fig. 2. CFD Computational domain: (a) inner rotating domain, (b) outer stationary domain.

B. Fluctuating Wind Simulation

The computational domains generated were imported into the CFD code FLUENT v14.5 for numerical iterative solution. The rotational motion was simulated by allowing the rotor sub-grid to rotate at constant angular velocity. The mesh movement was defined explicitly by specifying time-varying positions for all the rotor sub-grid block cell vertices. An interface boundary surrounding the rotating sub-grid within the model was allowed to slide at specified velocity to represent its relative motion to the stationary sub-grid.
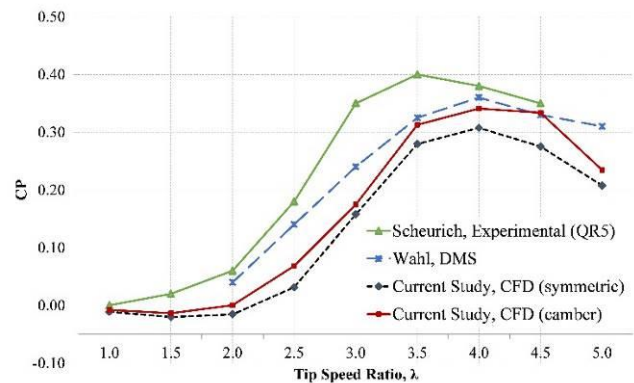

Fig. 3. CP curves vs. λ of various NACA XX25-bladed VAWTs.

The coupled pressure–based solver was selected with a second order implicit transient formulation for improved accuracy. All solution variables were solved using second order upwind discretization scheme since most of the flow can be assumed to be not in line with the mesh.

Fluctuating wind simulations were carried out by specifying the magnitude of the velocity inlet as a time-dependent variable. Specifically, the inlet boundary condition was set to a mean wind speed of U_{mean} = 5 m/s with fluctuating amplitude of U_{amp} = ±10% (±0.5m/s). Simulations were initially carried out at fluctuation frequencies f_c = 0.5Hz and f_c = 1Hz but was later determined that varying the unsteady wind f_c induced insignificant effect to VAWT performance, hence discussions were limited on comparing the results from one f_c case (f_c = 1Hz). The rotor angular speed is a constant ω = 13.33 rad/s that is the angular speed at λ = 4 where the optimum CP of VAWT in the steady wind case was achieved.

The total number of VAWT rotations under gust to complete one full wind cycle can be computed by the following notations as suggested by McIntosh et al. [12].

$$n_{rev} = \frac{\lambda_{mean}}{\pi k_{gust}} \qquad (1)$$

where n_{rev} is the number of rotor rotations in one wind cycle, λ_{mean} is the mean tip speed ratio computed from the varying values of ω as a response to unsteady U_∞ given by $\lambda_{mean} = \omega_{mean}R/U_{mean}$ and k_{gust} is the reduced gust frequency equal to $2R/D_g$. D_g is the variation in wind speed experienced by the VAWT during a gust and is equal to U_{mean}/f_c. Hence, k_{gust} formula can be rewritten to $k_{gust} = 2Rf_c/U_{mean}$.

For VAWT simulations with inlet boundary conditions set at U_{mean} = 5 m/s, fluctuating amplitude U_{amp} = ±10% (±0.5m/s) and fluctuation frequency f_c = 1Hz, the gust length D_g is 5 m. The mean tip speed ratio is $λ ≈ 4.02$, hence completing one wind cycle with about 2.13 rotations at a constant VAWT rotational speed of $ω$ = 13.33 rad/s. To ensure that a fully converged set of adjacent solutions is attained, a total of 21 full rotor rotations were simulated for each unsteady wind case.

III. RESULTS

A. Variation of T_b, $λ$ and $α$ in fluctuating $U_∞$

The T_b curves of all three blades over 21 rotations, together with the fluctuating wind stream, are shown in Fig. 4. As illustrated in the figures, the first three rotations of the VAWT showed unconverged set of T_b as reflected by the erratic trend of torque curves within the said range. The results were similar to that of the steady wind case where full convergence per time step was achieved only after several rotor rotations when residuals of all conserved variables were observed to fall below $1 × 10^{-4}$. To complete 21 rotor rotations, a total of about 564 processor hours was required for each run of unsteady wind simulation using an Intel–based computer with 4 cores of Intel® Core™ i7-3770 3.40GHz processors.

The torque produced at each blade for all test cases are observed to be mostly positive in magnitude. This indicates a positive overall performance of the VAWTs.

To illustrate and explain the VAWT performance under fluctuating wind, the focus of the succeeding discussions are the fully converged data generated from the last complete gust period. As seen in Fig. 5, approximately two rotor rotations is needed to complete one wind cycle with fluctuation frequency f_c = 1Hz, which supports the results from equation (1). Hence, rotor cycles 17th to 19th were considered.
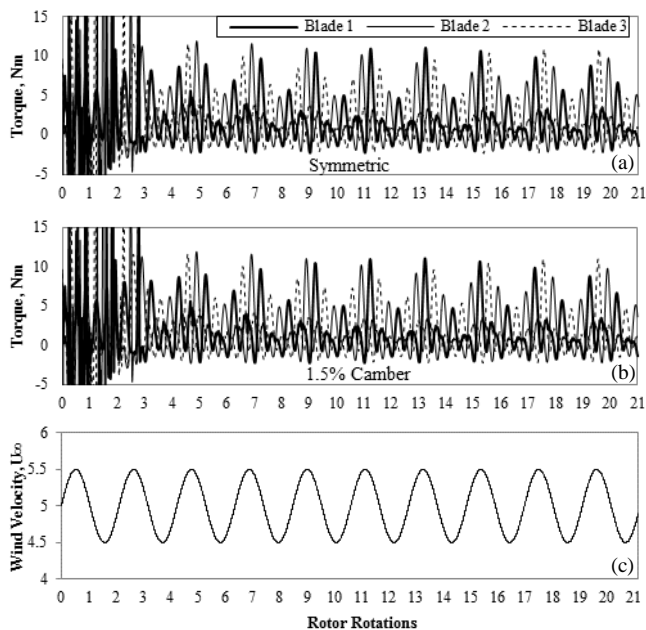
Fig. 4. Unsteady T_b and $U_∞$ curves over 21 VAWT rotations: (a) symmetric airfoil, (b) cambered airfoil, and (c) wind velocity.

At constant $ω$, an inverse relationship is observed between $λ$ and the fluctuating $U_∞$. An increase in $U_∞$ induces a corresponding decrease in $λ$. Having a U_{mean} = 5 m/s and a fluctuating amplitude set to 10%, the maximum $U_∞$ reaches up to 5.5 m/s and a minimum of 4.5 m/s. The maximum $U_∞$ was recorded at the middle of the first rotor cycle with a corresponding minimum $λ$ = 3.64. The maximum $α$ within the range of increasing $U_∞$ were recorded at ±15.68°. Depending on the blade on subject, the values occur within the first rotor cycle at 1Hz unsteady wind. The minimum $U_∞$, on the other hand, occurs at the middle of the second rotor cycle with a corresponding maximum $λ$ = 4.44. For this range, extreme values of $α$ were recorded at ±13.20° depending which blade is considered.
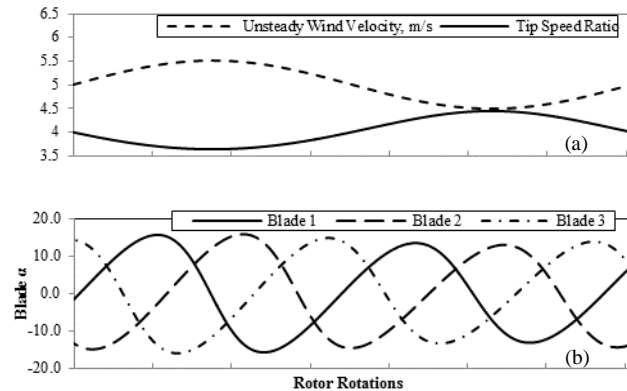
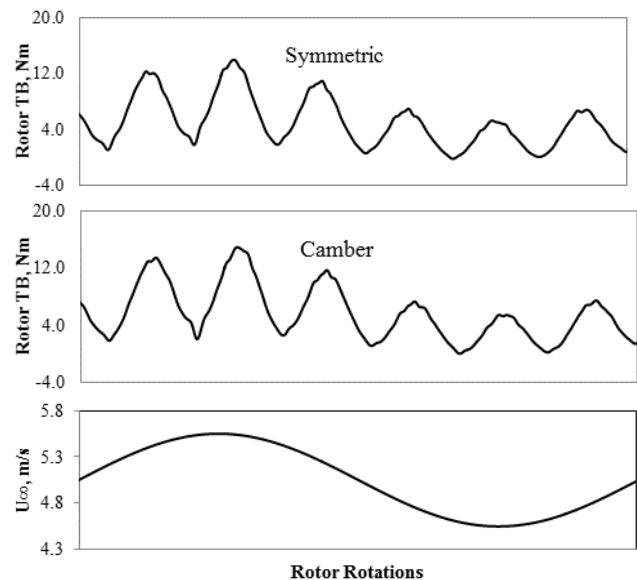Fig. 5. Variation in one wind cycle: (a) $U_∞$ and $λ$, (b) $α$.

Fig. 6. Variation of total rotor torque with $U_∞$.

The variation of the total combined torques T_B of VAWTs, with the fluctuating wind velocity $U_∞$ at U_{amp} = 10% and at f_c = 1Hz is shown in Fig. 6. As illustrated, similar to the individual torque T_b of each blade of the VAWT, the total combined torque T_B follows a positive trend with the increasing wind velocity. The maximum combined torques were computed to be 13.99 Nm and 14.78 for the symmetric and 1.5%-cambered blade, respectively, both occurring within the first rotor cycle where the maximum $U_∞$ was also recorded.

B. Variation of Power and C_P in fluctuating U_∞

Wind power P_W and rotor power P_B data, together with the resultant C_P for one wind cycle are illustrated in Fig. 7. Rotor power depends primarily on the magnitude of torque produced by the blades, hence was expected to show the same trend as that of the total torque curve with respect to the intensity of wind. P_B also increases with the increasing wind velocity U_∞ and wind power P_W, just like the total combined torque curve does. At $f_c = 1$Hz, the maximum P_B was computed at 186.33 Watts for the symmetrically bladed VAWT and 198.99 Watts for the camber-bladed VAWT occurring at the point of rotation where the P_W was recorded high with a value of around 304 Watts. Unsteady wind results show conformity with the steady wind results in terms of which VAWT configuration performed better in relation to the magnitude of the power output. The power generated by the 1.5% camber-bladed VAWT was predicted to be comparatively higher than that of the symmetric-bladed VAWT, marking a 6.36% difference between these two P_B values.

The instantaneous unsteady C_P curves of the symmetric and camber-bladed VAWT for said case are also illustrated in Fig. 7. These curves were consequently fitted with their corresponding quasi-steady C_P trend lines. It is apparent from the graph that the camber-bladed VAWT performs better with its instantaneous C_P curve on top of that of the symmetric-bladed VAWT, all throughout one wind cycle. A constant C_P difference of about 0.03 to 0.05 can also be observed between the quasi-steady curves of the two VAWT profiles. The difference in instantaneous C_P magnitude is computed at 11%, in favour of the VAWT with camber blades.

The cycle-averaged wind power was computed to be equal to 233.13 Watts. This value, together with the computed average P_B, was subsequently used to compute for the cycle-averaged power coefficients. The cycle-averaged P_B, P_W and C_P of all test cases from the unsteady wind simulations, together with the steady wind results, were computed and tabulated in Table 1. Similar to steady wind data, the VAWT with cambered airfoils generated higher power in unsteady wind – 74.96 Watts versus 66.92 Watts of the symmetrically bladed VAWT. This is also reflected in the computed cycle-averaged C_P (0.31 at $\lambda_{mean} = 4.02$) for the camber-bladed VAWT, that is higher compared to the computed cycle-averaged C_P of 0.28 ($\lambda_{mean} = 4.02$) for the symmetrically bladed VAWT.

On the other hand, by comparing these unsteady results to the steady wind data, it can be generalized that unsteady wind could have a detrimental effect to the performance of VAWT. As can be seen from the table, the cycle-averaged unsteady C_P of the camber-bladed VAWT is lower than the maximum C_P of the same VAWT profile in steady wind. A 9% drop in C_P from 0.34 ($\lambda = 4$) to 0.31 ($\lambda = 4.02$) was recorded. The rea-son behind this drop in C_P can be attributed to the poorer performance of the rotor in unsteady wind despite a higher value of recorded cycle-averaged wind power. Cycle-averaged unsteady rotor powers were computed to be equal to 66.92 Watts (symmetric) and 74.96 Watts (camber) at a cycle-averaged wind power of 233.13 Watts, versus the averaged steady rotor powers of 70.63

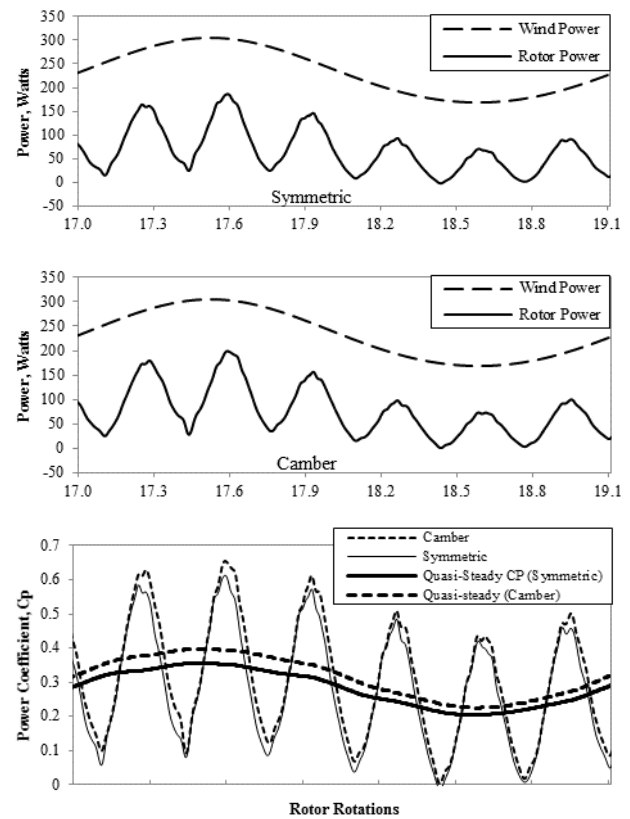Watts (symmetric) and 78.32 Watts (camber) at a constant 229.69 Watts wind power.

Fig. 7. Variation of power and C_P through one wind cycle.

Table I. Steady and unsteady VAWT performance

Wind Condition	Test Cases	Mean Rotor Power, W	Mean Wind Power, W	Mean C_P	λ_{mean}
Uniform Wind	Symmetric	70.63	229.69	0.31	4.00
	Camber	78.32	229.69	0.34	4.00
Fluctuating Wind	Symmetric	66.92	233.13	0.28	4.02
	Camber	74.96	233.13	0.31	4.02

IV. CONCLUSION

Results showed that VAWT power output and C_P increases with increasing wind velocity at a constant ω as observed from the quasi-steady curves fitted to the instantaneous data of these variables. However, comparing results between the two wind conditions, fluctuating wind imposed a detrimental effect to VAWT performance. The cycle-averaged unsteady C_P was lower than the maximum C_P computed from the steady wind case, for a specific VAWT profile. A 9% drop in C_P from 0.34 ($\lambda = 4$) to 0.31 ($\lambda = 4.02$) was recorded for the cambered-bladed VAWT, for instance. Despite the fact that a higher value of cycle-averaged wind power was recorded, the VAWTs performed poorer in unsteady wind. Cycle-averaged unsteady rotor powers were computed to be equal to 66.92 Watts (symmetric) and 74.96 Watts (camber) at a cycle-averaged wind power of 233.13 Watts, versus the averaged steady rotor powers of 70.63 Watts (symmetric) and 78.32 Watts (camber) at a constant 229.69 Watts wind power. The reason behind this is that

though higher blade torques were generated during the first half of the wind cycle due to the increased wind speeds at this range, this was counteracted by the lower torques generated at the second half of the wind cycle. Nevertheless, for the fluctuating wind condition, better performance was achieved by the camber-bladed VAWT as compared to the symmetric-bladed VAWT.

NOMENCLATURE

Symbol	Definition
c	blade chord
C_P	power coefficient
D_g	gust length
f_c	characteristic frequency of unsteady wind
k_{gust}	reduced gust frequency
k–ω SST	variant of k–ω turbulence model by Menter (1993)
n_{rev}	number of revolutions per wind cycle
P_B	blade power (three blades)
P_w	wind power
R	rotor radius
T_b	blade torque (single blade)
T_B	blade torque (three blades)
U_∞	free stream wind speed
U_{amp}	amplitude of fluctuation of unsteady wind
U_{mean}	mean speed of unsteady wind
y^+	dimensionless wall distance
α	angle of attack
ΔC_P	change in C_P
θ	azimuth position
λ	tip speed ratio, $R\omega/U_\infty$
λ_{mean}	tip speed ratio corresponding to ω_{mean}
μ_f	dynamic viscosity of fluid
ω	Instantaneous rotor angular speed
ω_{mean}	mean of ω
CFD	Computational Fluid Dynamics
DMS	double multiple streamtube model
HAWT	horizontal axis wind turbine
LES	large eddy simulation
RANS	Reynolds Averaged Navier–Stokes

REFERENCES

[1] Baker, J. R., 1983, "Features to Aid or Enable Self-Starting of Fixed Pitch Low Solidity Vertical Axis Wind Turbines," Journal of Wind Engineering and Industrial Aerodynamics, 15(1–3), pp. 369–380. ISSN 0167-6105, http://dx.doi.org/10.1016/0167-6105(83)90206-4.

[2] Christener, M., Dobbins, R., Ndegwa, A. and Sivak, J., 2010, "Rooftop Wind Turbine Feasibility in Bos-ton, Massachusetts," Report, Worcester Polytechnic Institute, May 2010, https://www.wpi.edu/ Pubs/E-project/Available/E-project-050410-163916/, accessed 23 June 2015.

[3] Mertens, S. and Van Bussel, G., 2003, "Performance of an H-Darrieus in the Skewed Flow on a Roof," Journal of Solar Engineering, 125(4), pp. 433–440. doi:10.1115/1.1629309.

[4] Kozak, P., 2014, "Effects of unsteady aerodynamics on vertical-axis wind turbine performance", Master's Thesis, Illinois Institute of Technology, June 2014, http://mypages.iit.edu/~pkozak/kozak_thesis_completed.pdf, accessed 23 June 2015.

[5] McIntosh, S. C., Babinsky, H. and Bertenyi, T., 2007, "Optimizing the Energy Output of Vertical Axis Wind Turbines for Fluctuating Wind Conditions", 45th AIAA Aerospace Sciences Meeting and Exhibit, Reno, Nevada, USA.

[6] Scheurich, F. and Brown, R. E., 2013, "Modelling the aerodynamics of vertical-axis wind turbines in unsteady wind conditions", Wind Energy, 16(1), pp. 91–107.

[7] Danao, L. A. M., 2012, "The Influence of Unsteady Wind on the Performance and Aerodynamics of Vertical Axis Wind Turbines", Ph.D. Thesis, The University of Sheffield, UK.

[8] Shahzad, A., Asim, T., Mishra, R., Paris, A., 2013, "Performance of a Vertical Axis Wind Turbine under Accelerating and Decelerating Flows", Procedia CIRP, 11(0), pp. 311-316, ISSN 2212-8271, http://dx.doi.org/10.1016/j.procir.2013.07.006.

[9] Raciti Castelli, M., Englaro, A., and Benini, E., 2011, "The Darrieus Wind Turbine: Proposal for a New Performance Prediction Model Based on CFD", Energy, 36(8), pp. 4919-4934.

[10] Scheurich, F., Fletcher, T. M., and Brown, R. E., 2010, "The Influence of Blade Curvature and Helical Blade Twist on the Performance of a Vertical-Axis Wind Turbine", 48th AIAA Aerospace Sciences Meeting Including the New Horizons Forum and Aerospace Exposition, Orlando, Florida, USA.

[11] Wahl, M., 2007, "Designing an H-rotor Type Wind Turbine for Operation on Amundsen-Scott South Pole Station", M.S. Thesis, Department of Engineering Sciences, Uppsala University, Sweden.